

© 2023 ELSEVIER. Personal use of this material is permitted. Permission from ELSEVIER must be obtained for all other uses, including reprinting/republishing this material for advertising or promotional purposes, collecting newly collected works for resale or redistribution to servers or lists, or reuse of any copyrighted component of this work in other works. This work has been submitted to the ELSEVIER for possible publication. Copyright may be transferred without notice, after which this version may no longer be accessible.

arXiv:2311.15843v1 [eess.SY] 27 Nov 2023

# Robust observer-based control with modularity and exponential stability for interconnected systems\*

Mehdi Heydari Shahna, Mohammad Bahari, Jouni Mattila

**Abstract**—This article introduces a modular robust subsystem-based adaptive (RSBA) control design with a new stability analysis for a class of uncertain interconnected systems with unknown modeling errors and interactions. First, we propose a nonlinear state observer for this class of systems that ensures uniformly exponential convergence of the estimation error by utilizing a new adaptive term, extending the conventional continuous Luenberger concept. Second, we introduce a novel adaptive subsystem-based control strategy for trajectory tracking, which incorporates an interesting term called the ‘stability connector,’ designed to capture dynamic interactions among subsystems during stability analysis, preventing excessive complexity as the system order increases. This represents the first instance of this term allowing modular control with exponential and uniform convergence rates, effectively handling unknown non-triangular nonlinearities. In addition to rigorous theoretical proofs by the Lyapunov theory, two complex systems are explored in simulations to confirm the merits of the suggested control schemes.

**Index Terms**—Subsystem-based control, adaptive control, uniformly exponential stability, modular control, nonlinear control.

## I. INTRODUCTION

Observers that exclusively use output, input, or existing knowledge of a system’s structure, or a combination thereof, can be a viable alternative for reducing the costs and noises associated with sensor usage [1]. Conversely, the systems in practice are susceptible to undesired influences that arise from various sources, such as external loads, fluctuations in temperature, humidity, noise, vibrations, the power supply, imprecise measurements, or the understanding of specific components’ behaviors, highlighting the crucial significance of designing robust control structures to avoid serious consequences [2]. Hence, Jiang et al. [3], for example, present an extended-state observer incorporating an adaptive bandwidth to enhance the dynamic performance. Likewise, in a study conducted by Guo et al. [4], an extended-state observer with backstepping was introduced to an electro-hydraulic system. Further, Din et al. [5] proposed a novel approach to designing nonlinear observers for estimating unknown disturbances. While all the mentioned papers achieve asymptotic convergence for the observer, which has become increasingly common recently [6]–[8], they do not provide information about the speed of the convergence. Furthermore, recent studies have not adequately addressed the nonlinear exponential state

observer. Hence, by providing reliable state information, the exponential observer serves as a fundamental basis for a robust controller, which is supposed to regulate and manipulate the behavior of a dynamic system to achieve desired outcomes in the presence of uncertainties and disturbances [9], [10].

In addition, employing different methods to decompose a complex system into subsystems can aid in developing a local control approach and in evaluating stability at the subsystem level, which facilitates control-based design and analysis [11], [12]. However, in most research findings, the functions bounding modeling errors and interactions are required to meet the triangular condition [13]–[15]. For instance, all control strategies, as presented in [16]–[19], were designed for systems with triangular uncertainty structures. This form of the system does not withhold all practical applications, and the triangular structural uncertainties may not be overcome by real-world interconnected systems, given that the bounding functions could rely on all state variables [13]. Likewise, Koivumaki et al. [20] employed a generic term (stability connector) to oversee interactions among subsystems with triangular structural uncertainties. Their interesting generic term facilitates modular control and prevents excessive complexity as the system order increases. This plays a vital role in defining the virtual stability of subsystems, leading to the stability of the entire system [12]. Conversely, Cai et al. [13] proposed a decentralized adaptive control scheme based on backstepping techniques for a class of interconnected systems. Their approach accommodated non-triangular uncertainties to achieve global boundedness, though it did not account for time-varying disturbances. Likewise, [21] proposed an adaptive neural control for non-triangular nonlinear systems with input delays, demonstrating that under bounded initial conditions, all signals in the closed-loop system remain bounded.

In this paper, we propose a novel robust subsystem-based adaptive (RSBA) control for a class of uncertain interconnected systems with unknown modeling errors and interactions. Our first objective is to extend the asymptotic conventional continuous Luenberger observer [22] by incorporating an additional adaptive term to achieve a uniformly exponential error reduction. While the observer strategies in [23], [24] are designed for triangular systems, the exponential observer developed in this paper expands this concept to a non-triangular system structure. Next, we introduce a novel robust subsystem-based control by developing a framework that builds on [20], which introduced an asymptotic ‘stability connector’ specifically designed for triangular systems

\*Funding for this research was provided by the Business Finland partnership project “Future All-Electric Rough Terrain Autonomous Mobile Manipulators” (Grant No. 2334/31/2022).

All authors are with Faculty of Engineering and Natural Sciences, Tampere University, Finland {Mehdi.heydarishahna, Mohammad.Bahari, Jouni.mattila}@tuni.fi

without unknown modeling errors. Our framework addresses the complex issue of adjacent subsystems with unknown modeling errors and interactions that are not inherently triangular. Interestingly, this stability analysis yields uniformly exponential stability for the entire system.

The key findings of this research are as follows: (1) Expanding upon the work of [22], a nonlinear state observer is proposed, aiming to achieve uniformly exponential convergence for non-triangular systems. (2) Inspired by the work of Koivumaki et al. [20], the novel RSBA control brings a new stability analysis by utilizing a "stability connector" that effectively cancels out the instability among subsystems, leading to an exponentially stable analysis of the entire system. (3) To our current understanding, no outcomes based on the subsystem-based approach have been reported for such interconnected systems.

After this section, we delve into the necessary details of the proposed control design in Section 2. Section 3 covers the design of the nonlinear state observer and the suggested controller structure, as well as analyzes the exponential stability of the robust observer and the whole system using the new generic term. Finally, we provide a step-by-step summary of the RSBA control algorithm in this section. Subsequently, we conduct simulations on two distinct systems with non-triangular uncertainties in Section 4: an uncertain seven-order system and an electro-mechanical linear actuator (EMLA) system decomposed into four subsystems to illustrate the effectiveness of our proposed approach. Eventually, the paper is concluded in Section 5.

## II. PROBLEM AND PRELIMINARIES

To propose the control methodology, a nonlinear  $n$ -order system is shown below.

$$\begin{cases} \dot{x}_1(t) = A_1 x_2(t) + g_1(x) + F_1(x) + d_1(t) \\ \dot{x}_i(t) = A_i x_{i+1}(t) + g_i(x) + F_i(x) + d_i(t) \\ \dot{x}_n(t) = A_n u(t) + g_n(x) + F_n(x) + d_n(t) \end{cases} \quad (1)$$

where  $i \in [1, 2, 3, \dots, n]$ , and  $n \in \mathbb{N}$  represents the number of states in the system denoted by  $x = [x_1, x_2, \dots, x_n]^T$ . The control input is represented by  $u(t) : \mathbb{R} \rightarrow \mathbb{R}$ ,  $A_i \in \mathbb{R}$  is any non-zero coefficient,  $g_i(x) = \rho_i^\top \tilde{g}_i(x)$  is a known non-triangular functional term originated from a model of the system,  $F_i(x) = \bar{\rho}_i^\top \tilde{F}_i(x)$  represents unknown non-triangular uncertainties relying on all state variables and resulting from incomplete knowledge of system parameters or modeling inaccuracy, and  $d_i : \mathbb{R} \rightarrow \mathbb{R}$  is a time-variant disturbance with uncertain magnitudes and timings. For any  $k \in \mathbb{N}$ ,  $\rho_i \in \mathbb{R}^k$  and  $\bar{\rho}_i \in \mathbb{R}^k$  are known and unknown constant parameters and  $\tilde{g}_i : \mathbb{R}^n \rightarrow \mathbb{R}^k$  and  $\tilde{F}_i : \mathbb{R}^n \rightarrow \mathbb{R}^k$  are known and unknown state-variant functions, respectively. Therefore, by considering the output of the system, we can also demonstrate the system as follows:

$$\begin{aligned} \dot{x}(t) &= Ax(t) + Bu(t) + g(x) + K(x(t), t) \\ y(t) &= Cx(t) \end{aligned} \quad (2)$$

where  $A \in \mathbb{R}^{n \times n}$ ,  $B \in \mathbb{R}^n$ , and  $C \in \mathbb{R}^{1 \times n}$  are observable, assuming that  $g(x) = [g_1, \dots, g_n]^\top$  comprises known modeling nonlinearities.  $K(\cdot) : \mathbb{R}^n \times \mathbb{R} \rightarrow \mathbb{R}^n$  represents unknown uncertainties or nonlinearities and is sufficiently smooth and continuous, as well as comprised of systematic uncertainties  $F_i(\cdot)$  and external disturbances  $d_i$ . The model system, when subjected to external disturbances and internal uncertainties, generates the output signal  $y(t) : \mathbb{R} \rightarrow \mathbb{R}$ . Thus, it is essential to consider the following information before presenting the design of the suggested robust state observer and control mechanism.

**Assumption 1** [25] Assume that matrices  $A$  and  $C$ , as provided in (2), are observable. Then, a feedback gain matrix  $\alpha$ , belonging to  $\mathbb{R}^n$ , can be found such that  $\bar{A} = A - \alpha C$  is a Hurwitz matrix.

**Assumption 2** [25] Following Assumption 1, and because  $K(x(t), t)$  is bounded, we can assume any positive definite  $q \in \mathbb{R}^{n \times n}$  in the following equation:

$$-q = p\bar{A} + \bar{A}^\top p \quad (3)$$

to obtain a positive definite  $p \in \mathbb{R}^{n \times n}$  such that for all  $(y(t), t) \in \mathbb{R} \times \mathbb{R}$ , the subsequent condition is met:

$$\|p K(x(t), t)\| \leq \|C^\top\| \eta^* H(y(t), t) \quad (4)$$

where  $\|\cdot\|$  denotes the squared Euclidean norm,  $\eta^* \in \mathbb{R}^+$  is an unknown positive constant, and  $H(\cdot) : \mathbb{R} \times \mathbb{R} \rightarrow \mathbb{R}^+$  is a known continuous positive function.

**Definition 1** [26] For  $t \geq t_0$ , the system tracking error  $x_e$  is uniformly exponentially stable if the following condition is satisfied:

$$\|x_e\| = \|x - x_d\| \leq \bar{c}e^{-\alpha(t-t_0)}\|x(t_0)\| + \tilde{\mu} \quad (5)$$

where  $\bar{c}, \tilde{\mu}$ , and  $\alpha \in \mathbb{R}^+$  are positive constants.  $x(t_0)$  is any initial state vector, and  $x_d$  is the reference trajectory. More precisely,  $x_e$  is uniformly exponentially stabilized within a defined region  $g(\tau)$ , as follows:

$$g(\tau) := \{x_e \mid \|x_e\| \leq \tau := \tilde{\mu}\} \quad (6)$$

## III. ROBUST SUBSYSTEM-BASED ADAPTIVE CONTROL

### A. Robust exponential state observer

After defining the error of state observation  $x_{eo} = x - \hat{x}$ , we can put forward an adaptive term in the following manner for the conventional Luenberger observer:

$$\begin{aligned} \dot{\hat{x}} &= A\hat{x} + Bu + g(x, t) + \alpha(y - \hat{y}) + p^{-1}C^\top f \\ \hat{y} &= C\hat{x}, \quad \bar{y} = y - \hat{y}, \quad \bar{y} = Cx_{eo} \\ \dot{x}_{eo} &= (A - \alpha C)x_{eo} + K(x(t), t) - p^{-1}C^\top f \end{aligned} \quad (7)$$

where  $\hat{x} : \mathbb{R} \rightarrow \mathbb{R}^n$  represents the estimated states. Furthermore, a finite and continuous function  $f(\cdot) : \mathbb{R} \times \mathbb{R} \rightarrow \mathbb{R}$  can be proposed as follows:

$$f(\bar{y}, \hat{\eta}(t), t) = \frac{\hat{\eta}^2 \cdot H(y, t)^2 \cdot \bar{y}}{\hat{\eta} H(y, t) \|\bar{y}\| + m(t)} \quad (8)$$

where  $m(t) : \mathbb{R} \rightarrow \mathbb{R}^+$  is a positive and continuous function constrained by the following condition:

$$\lim_{t \rightarrow \infty} \int_{t_0}^t m(T) dT \leq \bar{m} < \infty \quad (9)$$

$H(y, t)$  follows (4). The function  $\hat{\eta} : \mathbb{R} \rightarrow \mathbb{R}$  represents the adaptation law, as follows:

$$\dot{\hat{\eta}} = -m \ell \hat{\eta} + \ell H(y, t) \|\bar{y}\| \quad (10)$$

where  $\ell \in \mathbb{R}^+$ . If we define an unknown positive parameter, denoted by  $\eta^*$  in (4), and define the observer adaptation error system  $\bar{\eta} = \hat{\eta} - \eta^*$ , we obtain:

$$\dot{\bar{\eta}} = -m \ell \bar{\eta} + \ell H(y, t) \|\bar{y}\| - m \ell \eta^* \quad (11)$$

**Remark 1** As  $\hat{\eta}(t_0) > 0$ , according to (10), we can say  $\hat{\eta}(t) > 0$ . In addition, as with (8), we can say that  $f(\bar{y}, \hat{\eta}(t), t)$  can be:

$$\|f(\bar{y}, \hat{\eta}(t), t)\| \leq \hat{\eta} H(y(t), t) \quad (12)$$

### B. Modular control design

Our next step is to propose a controller structure that is compatible with the aforementioned observer. We can define the tracking error  $x_{e_i} \in \mathbb{R}$  as follows:

$$x_{e_i} = \hat{x}_i - x_{id}, \quad i = 1, \dots, n \quad (13)$$

Now, we transform the system into the form, as demonstrated in [27].

$$P_i = x_{e_i} - a_{i-1}, \quad P_0, a_0 = 0 \quad (14)$$

Let  $a_0 = 0$ .  $a_{i-1} : \mathbb{R} \rightarrow \mathbb{R}$  serves as a differentiable virtual control input and we define it for  $i = 1, \dots, n-1$ , as shown:

$$a_i = -\frac{1}{2A_i}(\beta_i + \zeta_i \hat{\theta}_i)P_i - \frac{A_{i-1}}{A_i}P_{i-1} - x_{(i+1)d} - \frac{1}{A_i}g_i \quad (15)$$

where  $A_0 = 0$ , and the adaptation parameter  $\hat{\theta}_i : \mathbb{R} \rightarrow \mathbb{R}$  is defined, as follows:

$$\dot{\hat{\theta}}_i = -\delta_i \sigma_i \hat{\theta}_i + \frac{1}{2} \zeta_i \delta_i |P_i|^2, \quad i = 1, \dots, n \quad (16)$$

where  $\delta_i$  and  $\sigma_i \in \mathbb{R}^+$ , and let  $\hat{\theta}_i(0) \geq 0$  be an initial condition for the adaptive system. Following Remark 1, we can have  $\hat{\theta}_i(t) > 0$ . Then, the subsequent function is introduced:

$$\bar{F}_i = F_i(x_1, \dots, x_n) - \left( \sum_{k=1}^n \frac{\partial a_{i-1}}{\partial x_k} \frac{dx_k}{dt} + \frac{\partial a_{i-1}}{\partial \hat{\theta}_{i-1}} \frac{d\hat{\theta}_{i-1}}{dt} + \frac{\partial a_{i-1}}{\partial x_{id}} \frac{dx_{id}}{dt} \right) \quad (17)$$

The smooth  $x_{id} \in \mathbb{R}$  is the reference trajectory for the subsystem  $i$ .

**Assumption 3** Let  $i = 1, \dots, n$ . Assume  $\bar{F}_i$ ,  $d_i$  and  $\dot{x}_{id}$  are bounded. Then, we can assume a positive smooth function  $r_i : \mathbb{R} \rightarrow \mathbb{R}^+$ , along with positive constants  $\Lambda_i$ ,  $d_{max(i)}$ , and

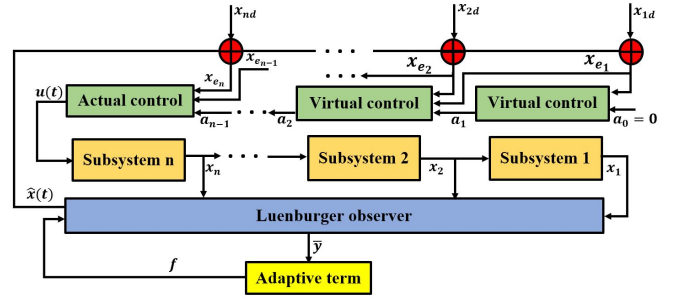


Fig. 1. Schematic of the RSBA control.

$\Omega_i \in \mathbb{R}^+$  exist, which may all be unknown, such that:

$$|\bar{F}_i| \leq \Lambda_i r_i, \quad |d_i| \leq d_{max(i)}, \quad |\dot{x}_{id}| \leq \Omega_i \quad (18)$$

Now, by differentiating (14), inserting (1) and (13) into it, and considering (17), we will have:

$$\dot{P}_i = A_i P_{i+1} + A_i x_{(i+1)d} + g_i + \bar{F}_i + A_i a_i + d_i - \dot{x}_{id}, \quad i = 1, \dots, n-1 \quad (19)$$

$$\dot{P}_n = A_n u(t) + g_n + \bar{F}_n - \dot{x}_{nd} + d_n$$

Similar to Eq. (15), we can propose the actual control input for (19), as follows:

$$u(t) = -\frac{1}{2A_n}(\beta_n + \zeta_n \hat{\theta}_n)P_n - \frac{A_{n-1}}{A_n}P_{n-1} - \frac{1}{A_n}g_n \quad (20)$$

where  $\zeta_i$ , and  $\beta_i$  are positive constants. We define the adaptation error  $\theta_i = \hat{\theta}_i - \theta_i^*$ , and we can obtain:

$$\dot{\theta}_i = -\delta_i \sigma_i \tilde{\theta}_i + \frac{1}{2} \zeta_i \delta_i |P_i|^2 - \delta_i \sigma_i \theta_i^* \quad (21)$$

where  $\theta_i^* \in \mathbb{R}^+$  is an unknown positive constant to tune the adaptation law and define, as follows:

$$\zeta_i \theta_i^* = \mu_i \Lambda_i^2 + \nu_i d_{max(i)}^2 + \psi_i (\Omega_i)^2 \quad (22)$$

where  $\mu_i$ ,  $\nu_i$ ,  $\psi_i$  and  $\Omega_i \in \mathbb{R}^+$  are unknown constants. Figure 1 demonstrates how the proposed controller operates.

### C. Stability analysis

**Theorem 1** Consider the uncertain interconnected systems outlined in (1) and (2), employing the modular RSBA control specified in (15) and (20) in conjunction with adaptive laws in (10) and (16). For any positive control gains satisfying (15), (20), (10), and (16), the trajectory tracking errors (13), and the state estimation error (7) converge to zero and the origin of the closed-loop error system is uniformly exponential stable.

**Proof** We introduce a Lyapunov function for the proposed observer in the following manner:

$$V_o = x_{eo}^\top p x_{eo} + \frac{1}{\ell} \bar{\eta}^2 \quad (23)$$

After taking the derivative of the Lyapunov function and

inserting (7), we have:

$$\begin{aligned} \dot{V}_o = & x_{eo}^\top [\bar{A}^\top p + p\bar{A}] x_{eo} + 2\ell^{-1}\bar{\eta}\dot{\bar{\eta}} \\ & + 2x_{eo}^\top p [K - p^{-1}C^\top f] \end{aligned} \quad (24)$$

Furthermore, (4) implies that for all  $t \geq t_0$ :

$$\begin{aligned} \dot{V}_o \leq & -x_{eo}^\top q x_{eo} + 2\eta^* H \|\bar{y}\| - 2x_{eo}^\top C^\top f \\ & + 2\ell^{-1}\bar{\eta}\dot{\bar{\eta}} \end{aligned} \quad (25)$$

Substituting Eqs. (8) and (11) into (25), we obtain:

$$\begin{aligned} \dot{V}_o \leq & -\bar{x}^\top q \bar{x} + 2\eta^* H \|\bar{y}\| - \frac{2\hat{\eta}^2 H^2 \|\bar{y}\|^2}{\hat{\eta} H \|\bar{y}\| + m} \\ & + 2\bar{\eta} H \|\bar{y}\| - 2m\bar{\eta}^2 - 2m\bar{\eta}\eta^* \\ = & -\bar{x}^\top q \bar{x} + \frac{2\hat{\eta} H \|\bar{y}\| \cdot m}{\hat{\eta} H \|\bar{y}\| + m} - 2m\bar{\eta}^2 - 2m\bar{\eta}\eta^* \\ = & -\bar{x}^\top q \bar{x} + \frac{2m(\hat{\eta} H \|\bar{y}\| + m) - 2m^2}{\hat{\eta} H \|\bar{y}\| + m} \\ & - 2m\bar{\eta}^2 - 2m\bar{\eta}\eta^* \end{aligned} \quad (26)$$

By analyzing Eq. (26) and eliminating the negative part from the right-hand side of (26), we have the option to deduce that:

$$\dot{V}_o \leq -\bar{x}^\top q \bar{x} + 2m - 2m\bar{\eta}^2 - 2m\bar{\eta}\eta^* \quad (27)$$

Then, according to Young's inequality, and considering  $-2\bar{\eta}\eta^* \leq \bar{\eta}^2 + \eta^{*2}$ , we obtain:

$$\begin{aligned} \dot{V}_o \leq & -\bar{x}^\top q \bar{x} + 2m - 2m\bar{\eta}^2 + m(\bar{\eta}^2 + \eta^{*2}) \\ = & -\bar{x}^\top q \bar{x} - m\bar{\eta}^2 + m(2 + \eta^{*2}) \end{aligned} \quad (28)$$

Hence, by knowing that  $p$  and  $q$  are positive definite matrices, we can assume there is a constant  $L \in \mathbb{R}$  in which:

$$-\bar{x}^\top q \bar{x} \leq -\bar{x}^\top p \bar{x} + L \quad (29)$$

Then:

$$\dot{V}_o \leq -\bar{x}^\top p \bar{x} - m\bar{\eta}^2 + m(2 + \eta^{*2}) + L \quad (30)$$

By considering  $\tilde{\mu}_o = (2 + \eta^{*2})$  and according to Young's inequality, we can reach:

$$\dot{V}_o \leq -\bar{x}^\top p \bar{x} - m\bar{\eta}^2 + L + \mu_{00}\tilde{\mu}_o^2 + \mu_{00}^{-1}m^2 \quad (31)$$

where  $\mu_{00}$  may be any positive constant. By defining the function  $\tilde{\mu} : \mathbb{R} \rightarrow \mathbb{R}$ , as follows:

$$\tilde{\mu} = \begin{cases} \mu_{00}\tilde{\mu}_o^2 + L & \text{if } L > 0 \\ \mu_{00}\tilde{\mu}_o^2 & \text{if } L \leq 0 \end{cases} \quad (32)$$

Therefore,  $\tilde{\mu}$  is always positive. From (23) and (32), we have (31), as follows:

$$\dot{V}_o \leq -\phi_o V_o + \mu_{00}^{-1}m^2 + \tilde{\mu} \quad (33)$$

where  $\phi_o = \min[1, \underline{m} \ell]$  and  $\underline{m} = \inf(m)$ . Now, a Lyapunov function for the first subsystem is proposed, as shown:

$$V_1 = \frac{1}{2} [P_1^2 + \delta_1^{-1}\tilde{\theta}_1^2] \quad (34)$$

After differentiating  $V_1$  and inserting (19), we obtain:

$$\begin{aligned} \dot{V}_1 = & A_1 P_1 P_2 + A_1 P_1 x_{2d} + P_1 g_1 + P_1 \bar{F}_1 + P_1 d_1 \\ & + A_1 P_1 a_1 - P_1 \dot{x}_{1d} + \delta_1^{-1} \tilde{\theta}_1 \dot{\tilde{\theta}}_1 \end{aligned} \quad (35)$$

Inspired by a fundamental principle in the virtual stability analysis (VDC), known as virtual power flow (VPF) [12], we employ an associated concept referred to as a stability connector between subsystems, as proposed by [20], [28]. The stability connector, for uncertain interconnected systems with unknown modeling errors and interactions provided in (1), can be defined, as follows:

$$S_i = A_i P_i P_{i+1}, \quad i = 1, \dots, n-1 \quad (36)$$

This term is a destabilizing dynamic interaction among subsystems in the process of stability. However, we will demonstrate that by utilizing this concept, we can introduce a new stability analysis that effectively offsets the instability of this term, leading to an exponentially stable analysis. By considering (18), (35), and using (36), we have:

$$\begin{aligned} \dot{V}_1 \leq & S_1 + A_1 P_1 x_{2d} + P_1 g_1 + |P_1| \Lambda_1 r_1 \\ & + |P_1| d_{\max(1)} + |P_1| \Omega_1 + A_1 P_1 a_1 \\ & + \delta_1^{-1} \tilde{\theta}_1 \dot{\tilde{\theta}}_1 \end{aligned} \quad (37)$$

By considering positive constants  $\psi_1$ ,  $\nu_1$  and  $\mu_1$ , and following Young's inequality, we have:

$$\begin{aligned} \dot{V}_1 \leq & S_1 + A_1 P_1 x_{2d} + P_1 g_1 + \frac{1}{2} |P_1|^2 \mu_1 \Lambda_1^2 \\ & + \frac{1}{2} \mu_1^{-1} r_1^2 + A_1 P_1 a_1 + \frac{1}{2} |P_1|^2 \nu_1 d_{\max(1)}^2 \\ & + \frac{1}{2} \nu_1^{-1} + \frac{1}{2} \psi_1 \Omega_1^2 P_1^2 + \frac{1}{2} \psi_1^{-1} + \delta^{-1} \tilde{\theta}_1 \dot{\tilde{\theta}}_1 \end{aligned} \quad (38)$$

By considering the description of  $\theta_1^*$  in (22), as well as the descriptions in (15) and (16), we obtain:

$$\begin{aligned} \dot{V}_1 \leq & S_1 + \frac{1}{2} \zeta_1 \theta_1^* |P_1|^2 + \frac{1}{2} \mu_1^{-1} r_1^2 + \frac{1}{2} \nu_1^{-1} \\ & - \frac{1}{2} \beta_1 P_1^2 + \frac{1}{2} \psi_1^{-1} - \frac{1}{2} \zeta_1 \hat{\theta}_1 P_1^2 - \sigma_1 \tilde{\theta}_1^2 \\ & + \frac{1}{2} \zeta_1 |P_1|^2 \tilde{\theta}_1 - \sigma_1 \theta_1^* \tilde{\theta}_1 \end{aligned} \quad (39)$$

Because  $\tilde{\theta}_1 = \hat{\theta}_1 - \theta_1^*$ :

$$\begin{aligned} \dot{V}_1 \leq & S_1 + \frac{1}{2} \mu_1^{-1} r_1^2 + \frac{1}{2} \nu_1^{-1} - \frac{1}{2} \beta_1 P_1^2 - \sigma_1 \tilde{\theta}_1^2 \\ & + \frac{1}{2} \psi_1^{-1} - \sigma_1 \theta_1^* \tilde{\theta}_1 \end{aligned} \quad (40)$$

After dividing  $\sigma_1 \tilde{\theta}_1^2$  into  $\frac{1}{2} \sigma_1 \tilde{\theta}_1^2 + \frac{1}{2} \sigma_1 \tilde{\theta}_1^2$  and considering (34), we can arrive at:

$$\begin{aligned} \dot{V}_1 \leq & -\phi_1 V_1 + S_1 + \frac{1}{2} \mu_1^{-1} r_1^2 + \frac{1}{2} \nu_1^{-1} + \frac{1}{2} \sigma_1 \theta_1^{*2} \\ & + \frac{1}{2} \psi_1^{-1} \end{aligned} \quad (41)$$

where:

$$\phi_1 = \min[\beta_1, \delta_1 \sigma_1] \quad (42)$$

Just as in (34), we present the same scenario for the  $j$ -th subsystem for  $j = 2, \dots, n-1$  subsystems by defining the Lyapunov function as follows:

$$V_j = \frac{1}{2} [P_j^2 + \delta_j^{-1} \tilde{\theta}_j^2] \quad (43)$$

By differentiating  $V_j$  and inserting (19), we have:

$$\begin{aligned} \dot{V}_j = & P_j [A_j P_{j+1} + A_j x_{(j+1)d} + g_j + \bar{F}_j + A_j a_j \\ & - \dot{x}_{jd} + d_j] + \delta_j^{-1} \tilde{\theta}_j \dot{\tilde{\theta}}_j \end{aligned} \quad (44)$$

Likewise, we continue by considering (15) and the stability connectors  $S_j, S_{j-1}$  from (36), inserted into (45), as follows:

$$\begin{aligned} \dot{V}_j = & S_j + P_j \bar{F}_j - \frac{1}{2} P_j (\beta_j + \zeta_j \hat{\theta}_j) P_j - S_{j-1} \\ & + P_j d_j - P_j \dot{x}_{jd} + \delta_j^{-1} \tilde{\theta}_j \dot{\tilde{\theta}}_j \end{aligned} \quad (45)$$

Similar to (35) to (42):

$$\begin{aligned} \dot{V}_j \leq & -\phi_j V_j + S_j - S_{j-1} + \frac{1}{2} \mu_j^{-1} r_j^2 + \frac{1}{2} \nu_j^{-1} \\ & + \frac{1}{2} \sigma_j \theta_j^{*2} + \frac{1}{2} \psi_j^{-1} \end{aligned} \quad (46)$$

where:

$$\phi_j = \min[\beta_j, \delta_j \sigma_j] \quad (47)$$

Likewise, we can establish an analogous Lyapunov function for the final subsystem, as shown:

$$V_n = \frac{1}{2} [P_n^2 + \delta_n^{-1} \tilde{\theta}_n^2] \quad (48)$$

By differentiating  $V_n$  and inserting (19), we have:

$$\begin{aligned} \dot{V}_n = & P_n [A_n u(t) + g_n + \bar{F}_n - \dot{x}_{nd} + d_n] \\ & + \delta_n^{-1} \tilde{\theta}_n \dot{\tilde{\theta}}_n \end{aligned} \quad (49)$$

Likewise, we continue by considering the control input provided in (20) and the stability connectors  $S_n$  from (36), inserted into (49), as follows:

$$\begin{aligned} \dot{V}_n \leq & -\phi_n V_n - S_{n-1} + \frac{1}{2} \mu_n^{-1} r_n^2 + \frac{1}{2} \nu_n^{-1} + \frac{1}{2} \psi_n^{-1} \\ & + \frac{1}{2} \sigma_n \theta_n^{*2} \end{aligned} \quad (50)$$

where:

$$\phi_n = \min[\beta_n, \delta_n \sigma_n] \quad (51)$$

Now, we introduce the Lyapunov function for the entire RSBA control system, as follows:

$$V = V_o + V_1 + \dots + V_j + \dots + V_n \quad (52)$$

After the derivative:

$$\dot{V} = \dot{V}_o + \dot{V}_1 + \dots + \dot{V}_j + \dots + \dot{V}_n \quad (53)$$

and after inserting (33), (41), (46), and (50) into (53), we obtain:

$$\begin{aligned} \dot{V} \leq & -\sum_{i=o}^n \phi_i V_i + \sum_{i=1}^{n-1} [-S_i + S_i] + \frac{1}{2} \sum_{i=1}^n \mu_i^{-1} r_i^2 \\ & + \frac{1}{2} \sum_{i=1}^n \nu_i^{-1} + \frac{1}{2} \sum_{i=1}^n \psi_i^{-1} + \frac{1}{2} \sum_{i=1}^n \sigma_i \theta_i^{*2} \\ & + \mu_{o0}^{-1} m^2 + \tilde{\mu} \end{aligned} \quad (54)$$

As we can observe in (54), based on the concept defined in (36), the non-triangular unstable term associated with dynamic interactions among subsystems has been effectively offset in this step. Now, we can transform the equations provided in (52) and (54), as follows:

$$V = \frac{1}{2} \mathbf{P}^\top \lambda \mathbf{P} + \frac{1}{2} \tilde{\theta}^\top \Delta^{-1} \tilde{\theta} \quad (55)$$

where:

$$\begin{aligned} \mathbf{P} = & \begin{bmatrix} x_{eo} \\ P_1 \\ \vdots \\ P_n \end{bmatrix}, \quad \lambda = \begin{bmatrix} 2p & 0 & 0 & \dots & 0 \\ 0 & 1 & 0 & \dots & 0 \\ \vdots & \vdots & \vdots & \vdots & \vdots \\ 0 & \dots & 0 & 0 & 1 \end{bmatrix}, \\ \tilde{\theta} = & \begin{bmatrix} \tilde{\eta} \\ \tilde{\theta}_1 \\ \vdots \\ \tilde{\theta}_n \end{bmatrix}, \quad \Delta^{-1} = \begin{bmatrix} 2\ell_1^{-1} & 0 & 0 & \dots & 0 \\ 0 & \delta_1^{-1} & 0 & \dots & 0 \\ \vdots & \vdots & \vdots & \vdots & \vdots \\ 0 & \dots & 0 & 0 & \delta_n^{-1} \end{bmatrix} \end{aligned} \quad (56)$$

Where  $\mathbf{P} : \mathbb{R}^n \times \mathbb{R}^n \rightarrow \mathbb{R}^{2n}$ ,  $\lambda : \mathbb{R}^{n \times n} \times \mathbb{R}^{n \times n} \rightarrow \mathbb{R}^{2n \times 2n}$ ,  $\tilde{\theta} : \mathbb{R} \times \mathbb{R}^n \rightarrow \mathbb{R}^{n+1}$ , and  $\Delta : \mathbb{R} \times \mathbb{R}^{n \times n} \rightarrow \mathbb{R}^{(n+1) \times (n+1)}$ . From (54), we can define:

$$\begin{aligned} \bar{\mu}^{-1} = & \max\left(\frac{2}{n} \mu_{o0}^{-1}, \tilde{\mu}_1^{-1}, \dots, \tilde{\mu}_n^{-1}\right) \\ M_i^2 = & m^2 + r_i^2 \\ \bar{\mu}_{total} = & \tilde{\mu} + \frac{1}{2} \sum_{i=1}^n \nu_i^{-1} + \frac{1}{2} \sum_{i=1}^n \psi_i^{-1} + \frac{1}{2} \sum_{i=1}^n \sigma_i \theta_i^{*2} \\ \phi_{total} = & \min[\phi_o, \phi_1, \dots, \phi_n] \end{aligned} \quad (57)$$

Then:

$$\dot{V} \leq -\phi_{total} V + \frac{1}{2} \sum_{i=1}^n \bar{\mu}^{-1} M_i^2 + \bar{\mu}_{total} \quad (58)$$

Thus, we can solve (58) as follows:

$$\begin{aligned} V \leq & V(t_0) e^{-\{\phi_{total}(t-t_0)\}} \\ & + \frac{1}{2} \bar{\mu}^{-1} \sum_{i=1}^n \int_{t_0}^t e^{-\{\phi_{total}(t-T)\}} M_i^2(T) dT \\ & + \bar{\mu}_{total} \int_{t_0}^t e^{-\{\phi_{total}(t-T)\}} dT \end{aligned} \quad (59)$$

Because  $e^{-\{\phi_{total}(t-t_0)\}}$  is always decreasing, we can interpret (59) as follows:

$$\begin{aligned} V \leq & V(t_0) e^{-\{\phi_{total}(t-t_0)\}} \\ & + \frac{1}{2} \bar{\mu}^{-1} \sum_{i=1}^n \int_{t_0}^t e^{-\{\phi_{total}(t-T)\}} M_i^2(T) dT \\ & + \bar{\mu}_{total} \phi_{total}^{-1} \end{aligned} \quad (60)$$

Based on (55) and according to (56), and defining  $\lambda_{min} \in \mathbb{R}$  as the minimum eigenvalue of matrix  $\lambda$ , we can say:

$$\begin{aligned} \|\mathbf{P}\|^2 &\leq \frac{2}{\lambda_{min}} V(t_0) e^{-\{\phi_{total}(t-t_0)\}} \\ &+ \frac{1}{\lambda_{min}} \bar{\mu}^{-1} \sum_{i=1}^n \int_{t_0}^t e^{-\{\phi_{total}(t-T)\}} M_i^2 dT \quad (61) \\ &+ \frac{2}{\lambda_{min}} \bar{\mu}_{total} \phi_{total}^{-1} \end{aligned}$$

Because  $\bar{\mu}$  may be any positive constant, we can express that:

$$\sum_{i=1}^n \frac{1}{\lambda_{min} \bar{\mu} \phi_{total}} < 1 \quad (62)$$

Therefore, we can presume a continuous function, as follows:

$$Z(\iota) = \sum_{i=1}^n \frac{\lambda_{min}^{-1} \bar{\mu}^{-1}}{\phi_{total} - \iota} > 0, \quad \iota \in [0, \phi_{total}] \quad (63)$$

Note that the initial quantity in (63) is equivalent to (62). It is now possible to assert that there exists a positive quantity  $\bar{\iota} \in \iota$ , such that:

$$0 \leq \bar{Z} = Z(\bar{\iota}) < 1 \quad (64)$$

By multiplying  $e^{\bar{\iota}(t-t_0)}$  to (61), we reach:

$$\begin{aligned} \|\mathbf{P}\|^2 e^{\bar{\iota}(t-t_0)} &\leq \frac{2}{\lambda_{min}} V(t_0) e^{-(\phi_{total}-\bar{\iota})(t-t_0)} \\ &+ \lambda_{min}^{-1} \bar{\mu}^{-1} \sum_{i=1}^n \int_{t_0}^t e^{-\phi_o(t-T)+\bar{\iota}(t-t_0)} M_i^2 dT \quad (65) \\ &+ \frac{2}{\lambda_{min}} \bar{\mu}_{total} \phi_{total}^{-1} e^{\bar{\iota}(t-t_0)} \end{aligned}$$

Because  $0 \leq \bar{\iota} < \phi_{total}$ , we can eliminate the decreasing element  $e^{-(\phi_{total}-\bar{\iota})(t-t_0)}$  from the right-hand side of (65):

$$\begin{aligned} \|\mathbf{P}\|^2 e^{\bar{\iota}(t-t_0)} &\leq \frac{2}{\lambda_{min}} V(t_0) \\ &+ \lambda_{min}^{-1} \bar{\mu}^{-1} \sum_{i=1}^n \int_{t_0}^t e^{-(\phi_{total}-\bar{\iota})(t-T)} \\ &M_i^2 e^{\bar{\iota}(T-t_0)} dT + \frac{2}{\lambda_{min}} \bar{\mu}_{total} \phi_{total}^{-1} e^{\bar{\iota}(t-t_0)} \end{aligned} \quad (66)$$

Using this approach, we can describe functions  $E_0$  and  $E_i$ , which are non-declining and continuous:

$$\begin{aligned} E_0 &= \sup_{e \in (t-t_0)} [\|\mathbf{P}\|^2 e^{\bar{\iota}(e-t_0)}] \\ E_i &= \sup_{e \in (t-t_0)} [(M_i^2) e^{\bar{\iota}(e-t_0)}] \end{aligned} \quad (67)$$

Next, by considering (66) and (67), and conducting some straightforward mathematical manipulations while removing the decreasing term, we obtain:

$$\begin{aligned} \|\mathbf{P}\|^2 e^{\bar{\iota}(t-t_0)} &\leq \frac{2}{\lambda_{min}} V(t_0) + \sum_{i=1}^n \frac{\lambda_{min}^{-1} \bar{\mu}^{-1}}{\phi_{total} - \bar{\iota}} E_i \\ &+ \frac{2}{\lambda_{min}} \bar{\mu}_{total} \phi_{total}^{-1} e^{\bar{\iota}(t-t_0)} \end{aligned} \quad (68)$$

As  $E_1$  does not exhibit a declining pattern, the left side of (68) will not exhibit a reduction. Therefore, with respect to the definition of  $E_0$  in (67), we can state that:

$$\begin{aligned} E_0 &\leq \frac{2}{\lambda_{min}} V(t_0) + \sum_{i=1}^n \frac{\lambda_{min}^{-1} \bar{\mu}^{-1}}{\phi_{total} - \bar{\iota}} E_i \\ &+ \frac{2}{\lambda_{min}} \bar{\mu}_{total} \phi_{total}^{-1} e^{\bar{\iota}(t-t_0)} \end{aligned} \quad (69)$$

Defining:

$$E = \max_i (E_i), \quad i = 0, \dots, n \quad (70)$$

we can have:

$$\begin{aligned} E_0 &\leq \frac{2}{\lambda_{min}} V(t_0) + \bar{Z} E \\ &+ \frac{2}{\lambda_{min}} \bar{\mu}_{total} \phi_{total}^{-1} e^{\bar{\iota}(t-t_0)} \end{aligned} \quad (71)$$

Because  $0 < E_0 \leq E$  and both  $E_0$  and  $E$  are non-declining, let us introduce  $\bar{Z}^*$ :

$$\bar{Z}^* > \bar{Z}, \quad 0 < \bar{Z}^* < 1 \implies \bar{Z} E \leq \bar{Z}^* E_0 \quad (72)$$

Eq. (72) is justified, as we can select  $\bar{\mu}$  such that  $\bar{Z}$  becomes sufficiently small in (63). When we incorporate (72) into (71), we arrive at:

$$\begin{aligned} E_0 &\leq \frac{2}{\lambda_{min}} V(t_0) + \bar{Z}^* E_0(t) \\ &+ \frac{2}{\lambda_{min}} \bar{\mu}_{total} \phi_{total}^{-1} e^{\bar{\iota}(t-t_0)} \end{aligned} \quad (73)$$

Afterward, we obtain:

$$E_0 \leq \frac{\frac{2}{\lambda_{min}} V(t_0) + \frac{2}{\lambda_{min}} \bar{\mu}_{total} \phi_{total}^{-1} e^{\bar{\iota}(t-t_0)}}{1 - \bar{Z}^*} \quad (74)$$

Concerning (67), we obtain:

$$\|\mathbf{P}\|^2 \leq \frac{\frac{2}{\lambda_{min}} V(t_0) e^{-\bar{\iota}(t-t_0)} + \frac{2}{\lambda_{min}} \bar{\mu}_{total} \phi_{total}^{-1}}{1 - \bar{Z}^*} \quad (75)$$

It is significant that:

$$\sup_{t \in [t_0, \infty]} \left( \frac{\frac{2}{\lambda_{min}} V(t_0) e^{-\bar{\iota}(t-t_0)}}{1 - \bar{Z}^*} \right) \leq \frac{\frac{2}{\lambda_{min}} V(t_0)}{1 - \bar{Z}^*} \quad (76)$$

Thus, based on Definition 1, it is obvious from (75) that, along with the adaptive algorithms provided in Eqs.(10), and (16) and the control input (20),  $\mathbf{P}$  including the state estimation error in (7), and the tracking error in (13) reach a defined region  $g_{total}(\bar{\tau}_0)$  in uniformly exponential convergence, such that:

$$g_{total}(\bar{\tau}_0) := \left\{ \|\mathbf{P}\| \leq \bar{\tau}_0 := \sqrt{\frac{\frac{2}{\lambda_{min}} \bar{\mu}_{total} \phi_{total}^{-1}}{1 - \bar{Z}^*}} \right\} \quad (77)$$

Therefore, we can conclude the demonstration of Theorem 1.

**Remark 2** As  $\bar{\mu}_{total}$ , consisting of  $\mu_{00}$ ,  $\tilde{\mu}_1, \dots$ , and  $\tilde{\mu}_n$ , and  $\lambda_{min}$ , resulted from  $p$ , can be chosen, it is possible to decrease the radius of the ball (77) as much as will satisfy (3), (62), and (72).

The deployment procedures for the RSBA control are described in **Algorithm**, which provides a summary and a step-by-step guide for implementing the RSBA control algorithm into n-order systems.

**Algorithm: RSBA control**

**Input:**  $y(t)$ ,  $A$ ,  $B$ ,  $C$ ,  $g_i$   
**Output:**  $u(t)$

```

1  While True do
2     $\alpha = \text{randn}(n, 1)$ ;
3     $\bar{A} = A - \alpha * C$ ;
4    If  $\bar{A}$  is Hurwitz, then
5      break;
6    end
7  end
8  While True do
9     $q = \text{randn}(n, n)$ ;
10    $q = q * q^T$ ;
11    $p = \text{lyap}(\bar{A}^T, q)$ ;
12   If all ( $\text{eig}(p) < 0$ ) then
13     break;
14   end
15    $\hat{\eta} = -m\ell\hat{\eta} + \ell H\|y - C\hat{x}\|$ .
16    $f = (\hat{\eta}^2 H^2 \bar{y}) / (\hat{\eta} H\|\bar{y}\| + m(t))$ .
17   For  $i = 1 : n$  do
18      $x_{e_i} = \hat{x}_i - x_{id}$ ;
19      $P_i = x_{e_i} - a_{i-1}$ ;
20      $\hat{\theta}_i = -\delta_i \sigma_i \hat{\theta}_i + \frac{1}{2} \zeta_i \delta_i |P_i|^2$ ;
21     If  $i \neq n$  then
22       obtain  $a_i$ ;
23     Else then
24       obtain  $u(t)$ ;
25     end
26   end
27   Repeat the steps from step 15 onward.
```

#### IV. NUMERICAL SIMULATION

In this section, we explore the effectiveness of our proposed algorithm through two distinct cases. Initially, we will analyze a complex seven-order system to illustrate the numerical reliability of the RSBA control approach confronted with diverse unknown modeling errors and interactions. As discussed in Section 1, many practical applications are characterized by non-triangular structural uncertainties. Therefore, in the second case, we explore an EMLA system equipped with a permanent magnet synchronous motor (PMSM), a practical example that includes non-triangular uncertainties and load disturbances affecting the system.

##### A. Seventh-order system

In the first case study, we build upon the study example presented by Yip et al. [29] and Koivunmaki et al. [20], who explored the potential of their proposed control approach in three-order and five-order systems with triangular forms of uncertainties. Based on the modeled dynamics, they assume all design uncertainties are known, except for some coefficient constants. In addition, they ignored the presence of external disturbances, which are only time-dependent. In

this paper, we investigate a more complicated system by increasing the order to seven ( $n = 7$ ), introducing additional unknown time-variant external disturbances  $d_i$ , and considering non-triangular uncertainties. Now, we investigate the potential of our proposed control method for the mentioned system, as described below:

$$\begin{aligned}
\dot{x}_1 &= 5x_1^3 x_2 + \cos(0.2t) + x_2 \\
\dot{x}_2 &= 5(x_5^2 + x_1^2 + x_4^2) + \sin(1.5\pi t) + x_3 \\
\dot{x}_3 &= 0.5x_1 x_2 x_3 - x_4 \\
\dot{x}_4 &= 10(x_1^2 x_4 - x_2^2 x_3) e^{-0.1t} - 2x_5 + 2e^{-0.1t} \\
\dot{x}_5 &= 5\sin^3(x_2) \sin(x_7) + x_6 - 5x_5 + 20 \\
\dot{x}_6 &= \arctan(x_6) e^{-3t} + 3x_1^2 - x_7 \\
\dot{x}_7 &= 0.5u + 20x_3 \arctan(x_4) e^{-2t} + \text{rand}(20) - x_2
\end{aligned} \tag{78}$$

where  $\text{rand}(20) \in \mathbb{R}$  is a function producing a random number between 0 and 20. Following step 2 of the algorithm, we assume:

$$\alpha = [1.32, 0.57, 1.13, -1.01, 0.75, 0.68, -0.93]^T \tag{79}$$

Then, after calculating the corresponding matrix  $\bar{A}$ , we can readily choose positive definite matrices by the MATLAB code *lyap* to identify matrices  $q$  and  $p$ , as step 11 of the algorithm. The function  $H(y(t), t)$  is defined as follows:

$$H(y(t), t) = 20 \cos(y)^4 + 20 \sin(y)^4 \tag{80}$$

Then, we choose:  $\ell = 1$ ,  $m = 200e^{-0.001t}$ . For the simulation, we will assign the starting conditions as follows:

$$\begin{aligned}
\hat{x}_0 &= [-1.2, -1.1, -0.8, -0.5, -0.3, -0.2, -1]^T, \\
\hat{\eta}(0) &= 1
\end{aligned} \tag{81}$$

Regarding the tracking error in step 19, we consider the reference trajectory  $x_{1d}$  as follows:

$$x_{1d} = \begin{cases} \tanh(t^3) \sin(2\pi t), & \text{if } t = 5 \\ \tanh(t^3) \sin(2\pi t) [1 - \tanh((t - 5))], & \text{else} \end{cases} \tag{82}$$

Furthermore, the control design parameters for this case study are outlined in Table I.

An important point to note is that in the sixth and seventh desired trajectories, there are significant amplitudes that occurred at the second 5, as shown in Fig. 2. As Fig. 2 indicates, the RSBA control can effectively perform trajectory tracking, even when confronted with unidentified nonlinearities. In summary, Table II presents a structural comparison of the approach introduced in this paper and the approach outlined in [20]. According to the table comparison, even though both studies proposed subsystem-based control methods and shared the same concept of dynamic interaction defined in Eq. (36) to eliminate unstable terms, an RSBA control could achieve exponential stability, a result stronger than that presented in [20]. Furthermore, in this paper, for the first case study, we considered a more complex system with a higher-order structure and a more intricate type of uncertainty (non-triangular), along with the presence of time-derivative

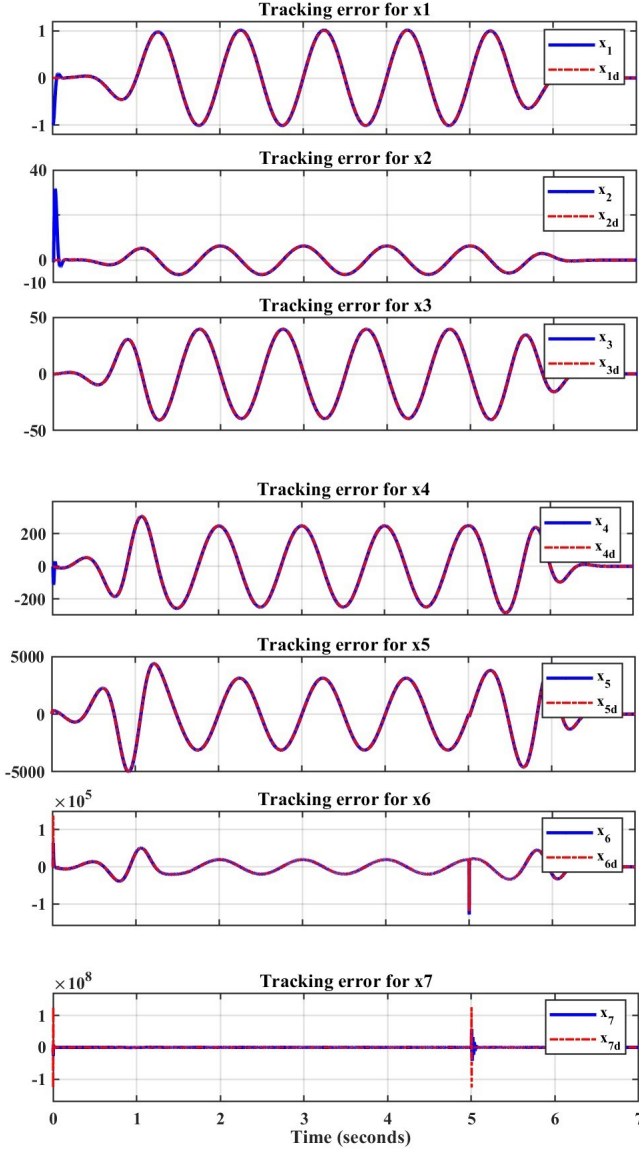


Fig. 2. Tracking error  $x_{e_i}$  for  $i = 1, \dots, 7$

disturbances.

### B. One-degree-of-freedom electro-mechanical linear actuator

In this section, we present an EMLA equipped with a PMSM as our practical system example with non-triangular nonlinearities, aiming to transform rotational motion into linear motion. The fundamental elements of an EMLA include a cylinder housing, attachments, a thrust tube, a ball screw or roller screw, a gearbox, and a motor (Fig. 3). The power transmission sequence of the EMLA commences with the motor, which generates torque and rotational speed through electrical power. The gearbox is responsible for decreasing the rotational speed while elevating the torque to the desired magnitude, whereas the screw shaft and nut assembly effectively convert the rotational motion into linear motion. The velocity and force of this linear motion maintain

TABLE I  
DESIGN PARAMETERS OF RSBA CONTROL.

$\beta_1 = 100$	$\zeta_1 = 0.1$	$\delta_1 = 0.1$	$\sigma_1 = 10$
$\beta_2 = 150$	$\zeta_2 = 1$	$\delta_2 = 1$	$\sigma_2 = 10$
$\beta_3 = 400$	$\zeta_3 = 1$	$\delta_3 = 1$	$\sigma_3 = 1$
$\beta_4 = 300$	$\zeta_4 = 10^{-2}$	$\delta_4 = 10^{-6}$	$\sigma_4 = 1$
$\beta_5 = 50$	$\zeta_5 = 10^{-6}$	$\delta_5 = 10^{-2}$	$\sigma_5 = 100$
$\beta_6 = 500$	$\zeta_6 = 10^{-8}$	$\delta_6 = 10^{-2}$	$\sigma_6 = 500$
$\beta_7 = 900$	$\zeta_7 = 10^{-9}$	$\delta_7 = 10^{-9}$	$\sigma_7 = 2 \times 10^3$

a proportional relationship with the screw lead, and the control procedure is executed within a rotating system based on the  $d$ - $q$  axis, followed by the implementation of Park transformations, to transform a three-phase (3-*Ph*) signal to the  $d$ - $q$  axis, as described in (83) and (84):

$$T = \begin{bmatrix} \cos(\omega t) & \cos(\omega t - \frac{2\pi}{3}) & \cos(\omega t + \frac{2\pi}{3}) \\ -\sin(\omega t) & -\sin(\omega t - \frac{2\pi}{3}) & -\sin(\omega t + \frac{2\pi}{3}) \\ \frac{1}{2} & \frac{1}{2} & \frac{1}{2} \end{bmatrix} \quad (83)$$

$$\begin{bmatrix} u_d \\ u_q \\ u_0 \end{bmatrix} = \frac{2T}{3} \begin{bmatrix} u_a \\ u_b \\ u_c \end{bmatrix} \quad (84)$$

The electrical characterization of the PMSM in the  $d$ - $q$  rotating reference frame is outlined in Eq. (85) within the context of the publication authored by Krishnan [30]:

$$\begin{aligned} \frac{di_q}{dt} &= \frac{1}{L_q} [u_q - R_s i_q - N_p \omega_m i_d L_d - N_p \omega_m \Phi_{PM}] \\ \frac{di_d}{dt} &= \frac{1}{L_d} [u_d - R_s i_d + N_p \omega_m i_q L_q] \end{aligned} \quad (85)$$

$$\tau_m = \frac{3}{2} N_p [i_q (i_d L_d + \Phi_{PM}) - i_d i_q L_q]$$

where  $L_d$  and  $L_q$  are the inductance and  $u_d$  and  $u_q$  are the voltages on the  $d$ - and  $q$ -axes. In addition,  $\omega_m$ ,  $R_s$ ,  $\Phi_m$ , and  $N_p$  are the mechanical rotational speed, phase resistance, permanent magnet flux, and number of rotor pole pairs, respectively. Regarding the mechanical components depicted in Fig. 3, the torque generated by the PMSM is transmitted to the gearbox and screw mechanism, respectively, and to simplify the rotary to linear motion conversion,  $\alpha_{RL}$  can be defined as (86):

$$\alpha_{RL} = \frac{2\pi}{\rho l} \quad (86)$$

Applying the principles of Newton's law of motion, we can deduce the torque balance equations for the PMSM ( $\tau_m$ ) and thereby achieve a comprehensive performance of an EMLA

TABLE II

COMPARISON OF RESULTS BETWEEN TWO MODULAR CONTROL METHODS WITH SUBSYSTEM STABILITY CONNECTOR.

method	uncertainty model	order	state availability	time-variant disturbances	stability
RSBA	non-triangular	7	exponential observer	✓	uniformly exponential
SBC [20]	triangular	5	assumed available	×	global asymptotic

system, as illustrated in (87):

$$\begin{cases} A_{eq} = \alpha_{RL} (J_m + J_c + J_{GB}) + \frac{1}{\alpha_{RL}\eta_{GB}} (M_{BS}) \\ B_{eq} = \alpha_{RL} (B_m) + \frac{1}{\alpha_{RL}\eta_{GB}} (B_{BS}) \\ C' = \left( \frac{1}{k_{\tau 1}} + \frac{1}{k_{\tau 2}} + \frac{1}{\rho^2 k_{\tau 3}} + \frac{\alpha_{RL}^2}{k_L} \right)^{-1} \\ C_{eq} = \alpha_{RL}^2 C' \\ D_{eq} = \frac{1}{\alpha_{RL}\eta_{GB}} \\ \tau_m = A_{eq} \ddot{x}_L + B_{eq} \dot{x}_L + C_{eq} x_L + D_{eq} F_L \end{cases} \quad (87)$$

where  $\rho$  and  $l$  are the gear ratio and lead of the screw. In addition,  $B_m$  and  $B_{BS}$  are the viscous friction of the electric motor and ball screw, accordingly. Further,  $J_m$ ,  $J_c$ , and  $J_{GB}$  are the motor, coupling, and gearbox inertia, and  $m_{BS}$  and  $\eta_{GB}$  are the ball screw mass and gearbox efficiency, respectively. Furthermore, the parameters  $k_{\tau 1}$ ,  $k_{\tau 2}$ , and  $k_{\tau 3}$  correspond to the stiffness attributes of the motor's shaft and coupling, gearbox, and screw shaft, respectively. Meanwhile, the parameter  $k_L$  denotes the collective linear stiffness encompassing the thrust bearing, ball screw, ball nut, and thrust tube components, and it can be calculated using (88):

$$k_L = \left( \frac{1}{k_{bearing}} + \frac{1}{k_{screw}} + \frac{1}{k_{nut}} + \frac{1}{k_{tube}} \right)^{-1} \quad (88)$$

In the context of the studied EMLA, the state vector  $x(t) \in \mathbb{R}^4$  and input vector  $u(t) \in \mathbb{R}^3$  for the state-space model of the studied EMLA can be defined as in (89):

$$\begin{cases} x(t) = [x_L(t) \quad \dot{x}_L(t) \quad i_q(t) \quad i_d(t)]^T \\ u(t) = [i_q^*(t) \quad u_q(t) \quad u_d(t)]^T \end{cases} \quad (89)$$

Ultimately, we can define the state space vector for the given case, as expressed in Eq. (90):

$$\begin{cases} \dot{x}_1 = x_2 \\ \dot{x}_2 = \frac{1}{A_{eq}} \left[ \frac{3}{2} N_p (x_3 x_4 L_d + i_q^* \Phi_{PM} - x_3 x_4 L_q) - B_{eq} x_2 - C_{eq} x_1 - D_{eq} F_L \right] \\ \dot{x}_3 = \frac{1}{L_q} [u_q - R_s x_3 - N_p \alpha_{RL} x_2 (x_4 L_d + \Phi_{PM})] \\ \dot{x}_4 = \frac{1}{L_d} [u_d - R_s x_4 + N_p \alpha_{RL} x_2 x_3 L_q] \end{cases} \quad (90)$$

Finally, the pulse width modulation (PWM) block generated the corresponding rectangular waveforms used to control the power switch S1–S6 of the inverter. Table IV provides an overview of the essential features of the components within

the EMLA system, including the motor, gearbox, and ball screw [31]:

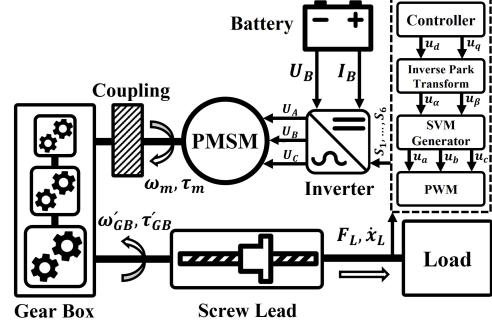


Fig. 3. One-degree of freedom EMLA mechanism

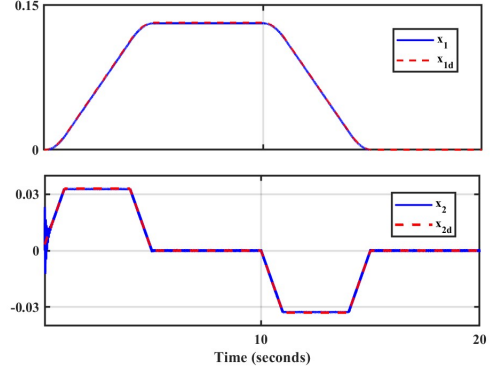


Fig. 4. Tracking error for linear position and velocity

As such, the order of the system is four, and by considering the RSBA control algorithm from step 1 to step 17, we can assume  $\alpha = [0.53, 1.83, -2.25, 0.86]^T$  and  $C = [1, 0, 1, 1]$ . Note that it is common to consider reference trajectories of the EMLA as  $x_{2d} = \dot{x}_{1d}$ ,  $x_{3d} = i_q^*$ , and  $x_{4d} = i_d^* = 0$ , following [35]. As shown, the control signal of the second subsystem  $i_q^*$  is the desired value for the third state  $x_3 = i_q$ . Therefore, after receiving the state values from the observer algorithm, we should adopt the transformation of the EMLA system and control algorithm from step 20. The control parameters for this case study are selected as  $\beta_i = 600$ ,  $\zeta_i = 0.001$ ,  $\delta_i = 0.001$ , and  $\sigma_i = 2000$  for  $i = 1, \dots, 4$ . As illustrated in Figs. 4 and 5, tracking errors of the linear position ( $x_1$ , in meters), velocity ( $x_2$ , in meters per second), and current states ( $x_3$  and  $x_4$ ), measured in ampere (A), have been attained in the face of non-triangular uncertainties and the same influence of external loads as the previous case study. For this case study, we are conducting a comparison

TABLE III  
COMPARISON OF RESULTS BETWEEN TWO CONTROL EMLA SYSTEMS

method	type of control	stability	observer
RSBA control [8] [33]	linear motion control angular position control torque and flux control	uniformly exponential asymptotic asymptotic	novel exponential observer Luenberger observer from [32] Kalman filter from [34]

TABLE IV  
CHARACTERISTICS OF THE EMLA PARAMETERS [31].

Symbol	Parameter	Value	Unit
$l$	Screw lead	16	mm
$\rho$	Gearbox ratio	0.0416	-
$\eta_{GB}$	Gearbox Efficiency	96	%
$N_p$	Pole pairs	2	-
$R_s$	Stator resistance	0.57	$\Omega$
$\Phi_{PM}$	PM flux	0.108	Wb
$L_d$	d-axis inductance	8.72	mH
$L_q$	q-axis inductance	22.8	mH
$u_{max}$	Maximum voltage	50	V
$i_{max}$	Maximum current	8.66	A
$A_{eq}$	Equivalent mass	$22 \times 10^4$	kg
$B_{eq}$	Equivalent damping	$\frac{\sqrt{A_{eq}C_{eq}}}{25}$	$\frac{N \cdot s}{m}$
$C_{eq}$	Equivalent stiffness	$4 \times 10^8$	N/m
$D_{eq}$	Mechanical	$1 \times 10^{-4}$	-
$F_L$	Efficiency Load	22	kN

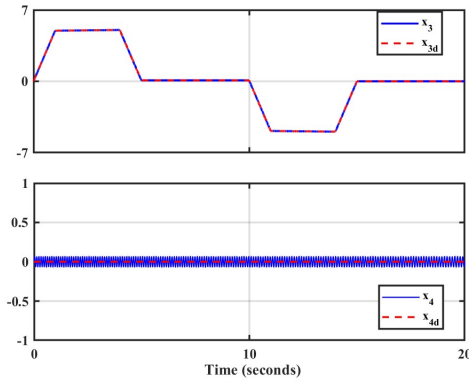


Fig. 5. Tracking error for currents

between this work and similar control studies on PMSMs, as listed in Table III. In contrast, references [8] and [33] focused solely on the angular motion of a motor, whereas our case dealt with a linear actuator equipped with a PMSM motor. Furthermore, the stability achieved by the RSBA control method utilized in our study surpassed theirs, demonstrating exponential stability as opposed to asymptotic stability. In addition, while their system information relied on previously worked asymptotic stable estimation algorithms from [32] and [34] to determine the state values, our paper introduced a novel exponential observer.

## V. CONCLUSION

This research study proposed a new modular RSBA control for a class of uncertain interconnected systems with unknown modeling errors and interactions. First, we achieved a nonlinear state observer with uniformly exponential convergence for this class of systems by expanding the conventional continuous Luenberger concept with an additional adaptive term. This observer can streamline future control efforts, particularly in applications requiring exponential convergence. Then, based on a robust subsystem-based adaptive approach, the proposed control method decomposed an n-order system, and it employed a new stability analysis approach. This strategy incorporates an interesting term called the ‘stability connector,’ designed to capture non-triangular dynamic interactions among subsystems that effectively offset the instability of the system, leading to an exponentially stable analysis for the entire system. This stability analysis sets the stage for future research efforts centered around subsystem-based methodologies.

## REFERENCES

- [1] Y. Wang, J. Tian, Z. Sun, L. Wang, R. Xu, and M. Li, “A comprehensive review of battery modeling and state estimation approaches for advanced battery management systems,” *Renewable and Sustainable Energy Reviews*, vol. 131, p. 110015, 2020.
- [2] C. Tsui, *Robust Control System Design: Advanced State Space Technique*. CRC Press, 2022.
- [3] F. Jiang, S. Sun, A. Liu, Y. Xu, Z. Li, X. Liu, and K. Yang, “Robustness improvement of model-based sensorless SPMSM drivers based on an adaptive extended state observer and an enhanced quadrature PLL,” *IEEE Transactions on Power Electronics*, vol. 36, no. 4, pp. 4802–4814, 2020.
- [4] Q. Guo, Y. Zhang, B. Celler, and S. Su, “Backstepping control of electro-hydraulic system based on extended-state-observer with plant dynamics largely unknown,” *IEEE Transactions on Industrial Electronics*, vol. 63, no. 11, pp. 6909–6920, 2016.
- [5] S. Ding, W. Chen, K. Mei, and D. Murray-Smith, “Disturbance observer design for nonlinear systems represented by input–output models,” *IEEE Transactions on Industrial Electronics*, vol. 67, no. 2, pp. 1222–1232, 2019.
- [6] Pan, J., Nguyen, A., Guerra, T., and Ichalal, D., “A unified framework for asymptotic observer design of fuzzy systems with unmeasurable premise variables,” *IEEE Transactions on Fuzzy Systems*, vol. 29, no. 10, pp. 2938–2948, 2021.
- [7] A. Rapaport and D. Dochain, “A robust asymptotic observer for systems that converge to unobservable states—a batch reactor case study,” *IEEE Transactions on Automatic Control*, vol. 65, no. 6, pp. 2693–2699, 2020.
- [8] Sun, X., Yu, H., Yu, J., and Liu, X., “Design and implementation of a novel adaptive backstepping control scheme for a PMSM with unknown load torque,” *IET Electric Power Applications*, vol. 13, no. 4, pp. 445–455, 2019.
- [9] Kundur, P. and Malik, O., *Power System Stability and Control*. McGraw-Hill Education, 2022.
- [10] Yedavalli, R. K., “Robust control of uncertain dynamic systems,” *AMC*, vol. 10, p. 12, 2014.
- [11] Vaidyanathan, S. and Azar, A. T., *Backstepping Control of Nonlinear Dynamical Systems*. Academic Press, 2020.

- [12] Zhu, W. H., *Virtual Decomposition Control: Toward Hyper Degrees of Freedom Robots*, ser. Advances in Industrial Control. Springer Science & Business Media, 2010, vol. 60.
- [13] Cai, J., Wen, C., Xing, L., and Yan, Q., “Decentralized backstepping control for interconnected systems with non-triangular structural uncertainties,” *IEEE Transactions on Automatic Control*, vol. 68, no. 3, pp. 1692–1699, 2020.
- [14] Zhang, X., *Strict-feedback nonlinear systems: gain control design*, Vol. 7. Springer Nature, 2023.
- [15] Tong, S. and Li, Y., “Observer-based fuzzy adaptive control for strict-feedback nonlinear systems,” *Fuzzy Sets and Systems*, vol. 160, no. 12, pp. 1749–1764, 2009.
- [16] Xing, L. and Wen, C., “Dynamic event-triggered adaptive control for a class of uncertain nonlinear systems,” *Automatica*, vol. 158, p. 111286, 2023.
- [17] Jiang, Y., Fan, J., Gao, W., Chai, T., and Lewis, F. L., “Cooperative adaptive optimal output regulation of nonlinear discrete-time multi-agent systems,” *Automatica*, vol. 121, p. 109149, 2020.
- [18] Wang, J., Li, J., He, C., and Liu, S., “Output regulation for the parametric strict-feedback system via the event-triggered adaptive updating algorithm,” *Applied Mathematical Modelling*, vol. 96, pp. 598–616, 2021.
- [19] Bernard, P., Bin, M., and Marconi, L., “Adaptive output regulation via nonlinear luenberger observer-based internal models and continuous-time identifiers,” *Automatica*, vol. 122, p. 109261, 2020.
- [20] Koivumäki, J., Humaloja, J. P., Paunonen, L., Zhu, W. H., and Mattila, J., “Subsystem-based control with modularity for strict-feedback form nonlinear systems,” *IEEE Transactions on Automatic Control*, 2022.
- [21] Wang, H., Liu, S., and Yang, X., “Adaptive neural control for non-strict-feedback nonlinear systems with input delay,” *Information Sciences*, vol. 514, pp. 605–616, 2020.
- [22] Marconi, L., Praly, L., and Isidori, A., “Output stabilization via nonlinear luenberger observers,” *SIAM Journal on Control and Optimization*, vol. 45, no. 6, pp. 2277–2298, 2007.
- [23] Zhai, D., An, L., Dong, J., and Zhang, Q., “Output feedback adaptive sensor failure compensation for a class of parametric strict feedback systems,” *Automatica*, vol. 97, pp. 48–57, 2018.
- [24] Zhang, C., Chang, L., Xing, L., and Zhang, X., “Fixed-time stabilization of a class of strict-feedback nonlinear systems via dynamic gain feedback control,” *IEEE/CAA Journal of Automatica Sinica*, vol. 10, no. 2, pp. 403–410, 2023.
- [25] Chen, Y., “Adaptive robust observers for non-linear uncertain systems,” *International Journal of Systems Science*, vol. 21, no. 5, pp. 803–814, 1990.
- [26] Loria, A. and Panteley, E., “Uniform exponential stability of linear time-varying systems: revisited,” *Systems & Control Letters*, vol. 47, no. 1, pp. 13–24, 2002.
- [27] Tong, S., Liu, C., and Li, Y., “Fuzzy-adaptive decentralized output-feedback control for large-scale nonlinear systems with dynamical uncertainties,” *IEEE Transactions on Fuzzy Systems*, vol. 18, no. 5, pp. 845–861, 2010.
- [28] Petrović, G. R. and Mattila, J., “Mathematical modelling and virtual decomposition control of heavy-duty parallel–serial hydraulic manipulators,” *Mechanism and Machine Theory*, vol. 170, p. 104680, 2022.
- [29] Yip, P. P. and Hedrick, J. K., “Adaptive dynamic surface control: A simplified algorithm for adaptive backstepping control of nonlinear systems,” *International Journal of Control*, vol. 71, no. 5, pp. 959–979, 1998.
- [30] Krishnan, R., (2017). *Permanent magnet synchronous and brushless DC motor drives*. CRC Press, 2017.
- [31] Väisänen, T., “(2023). *Simulation of electro-mechanically actuated boom*,” Master’s thesis, Tampere University.
- [32] Petrovic, V., Ortega, R., and Stankovic, A.M., “Interconnection and damping assignment approach to control of pm synchronous motors,” *IEEE Transactions on Control Systems Technology*, vol. 9, no. 6, pp. 811–820, 2001.
- [33] Z. Xu and M. F. Rahman, “An adaptive sliding stator flux observer for a direct-torque-controlled IPM synchronous motor drive,” *IEEE Transactions on Industrial Electronics*, vol. 54, no. 5, pp. 2398–2406, 2007.
- [34] Harnefors, L., “(1996). *Speed estimation from noisy resolver signals*, IET.”
- [35] Chai, S., Wang, L., and Rogers, E., “Model predictive control of a permanent magnet synchronous motor with experimental validation,” *Control Engineering Practice*, vol. 21, no. 11, pp. 1584–1593, 2013.